New Journal of Physics
The open access journal at the forefront of physics

Deutsche Physikalische Gesellschaft DPG
IOP Institute of Physics

Published in partnership with: Deutsche Physikalische Gesellschaft and the Institute of Physics

OPEN ACCESS

RECEIVED
19 January 2017

REVISED
27 April 2017

ACCEPTED FOR PUBLICATION
1 June 2017

PUBLISHED
8 September 2017

PAPER

Actin and microtubule networks contribute differently to cell response for small and large strains

H Kubitschke[1], **J Schnauss**[1,2], **K D Nnetu**[1], **E Warmt**[1], **R Stange**[1] and **J Kaes**[1]

[1] Peter Debye Institute for Soft Matter Physics, University Leipzig, Linnestraße 5, D-04103 Leipzig, Germany
[2] Fraunhofer Institute for Cell Therapy and Immunology, Perlickstraße 1, D-04103 Leipzig, Germany

E-mail: hans.kubitschke@uni-leipzig.de

Keywords: optical stretcher, actin filaments, microtubules, latrunculin A, jasplakinolide, nocodazole, paclitaxel

Supplementary material for this article is available online

Abstract

Cytoskeletal filaments provide cells with mechanical stability and organization. The main key players are actin filaments and microtubules governing a cell's response to mechanical stimuli. We investigated the specific influences of these crucial components by deforming MCF-7 epithelial cells at small ($\leqslant$5% deformation) and large strains (>5% deformation). To understand specific contributions of actin filaments and microtubules, we systematically studied cellular responses after treatment with cytoskeleton influencing drugs. Quantification with the microfluidic optical stretcher allowed capturing the relative deformation and relaxation of cells under different conditions. We separated distinctive deformational and relaxational contributions to cell mechanics for actin and microtubule networks for two orders of magnitude of drug dosages. Disrupting actin filaments via latrunculin A, for instance, revealed a strain-independent softening. Stabilizing these filaments by treatment with jasplakinolide yielded cell softening for small strains but showed no significant change at large strains. In contrast, cells treated with nocodazole to disrupt microtubules displayed a softening at large strains but remained unchanged at small strains. Stabilizing microtubules within the cells via paclitaxel revealed no significant changes for deformations at small strains, but concentration-dependent impact at large strains. This suggests that for suspended cells, the actin cortex is probed at small strains, while at larger strains; the whole cell is probed with a significant contribution from the microtubules.

1. Introduction

The ability of cells to sense and adapt to their environment plays a vital role in many of their biologically relevant functions. In the last decade, connections between the mechanical properties of cells and the initiation as well as progress of pathologies such as cancer [1, 2] have been made. These connections highlight the link between molecular changes within the cytoskeleton to morphological and functional changes of the entire cell. In this way, it has been shown that actin filaments and microtubules play significant roles in dynamic cellular processes such as proliferation [3], migration [4–6], differentiation, [7] and apoptosis [8]. Besides their dynamic functions, they lend cells mechanical stability and govern their responses against external, mechanical stimuli. During cancer metastasis, for instance, cells have to squeeze through the underlying extracellular matrix and vascular walls. Extravasation and intravasation during metastasis could lead to small or large deformation of the cells depending on the pore sizes of their surrounding environment. After extravasation, the single cells are transported in suspension to other parts of the body through the blood and spread through the lymph vessel [9].

The interaction between actin filaments and microtubules as well as their contribution to intracellular force balances have been discussed with respect to the traction forces exerted by cells on deformable substrates [10, 11]. These studies revealed the stress bearing ability of microtubules as well as the contractile forces produced by actin filaments together with myosin motors. It remains to be shown that such a force balance mechanism exists in suspended cells. The resistance of cells against deformations has been investigated via

techniques such as magnetic twisting cytometry (MTC) [12, 13], atomic force microscopy (AFM) [14, 15], laser tracking microrheology [13], hydrodynamic stretching with flow-cytometers [16–20], and optical stretcher (OS) [1, 21–24]. These studies were performed on various cell types [7, 25] and often indicate that actin filaments are a major contributor to the mechanical properties of cells. AFM-based studies further showed that microtubule stabilization or disruption did not affect cell elasticity [14, 25] or is only of minor importance [20]. In contrast, MTC studies revealed that destabilization of microtubules inhibited cell stiffness while stabilizing them led to increased cell stiffening [12]. Some of these studies, however, were performed on adherent cells and the measured mechanical properties depend on the local conditions rather than global characteristics [26]. Given the fact that a cell is spatially heterogeneous, the measured mechanical properties vary [13] and are not representative of the response of a cell as a whole to perturbation. In addition, it was shown that also keratin can play a major role in cell stiffness [27].

In contrast, whole cell deformations have been performed either by stretching cells using microplates [28, 29], or by micropipette aspiration [30]. Moreover, cells have been deformed by compression against a glass slide [31] or by use of optical forces such as the OS [7], including contractile force measurements [32], and optical tweezers [33], including force fluctuation measurements [34]. These studies also found that actin filaments are the major contributor to cell elasticity while microtubules contributed to cell relaxation [7]. At large strains, actin filaments have been shown to rupture in *in vitro* studies while the contribution of intermediate filaments and microtubules to cell elasticity becomes dominant [27, 35]. It has also been hypothesized via finite elements simulations [36] that microtubules contribute more to cell elasticity at large strains. Therefore, the disruption of microtubules at large strains has been shown to reduce the non-linearity in whole cell stiffness [37]. In most studies, cells are probed within a linear regime but the magnitude of the deformation (small or large) and its impact on the response of a cell as a whole has not been characterized. Here, we characterize the response of MCF-7 cells to optically applied forces at large and small strains by the means of the previously established automated microfluidic OS [22, 38, 39]. A low and high strain regime were established by employing step stress profiles generated by low and high laser powers. Additionally, target-specific drugs induced cytoskeletal perturbations and according changes in the relative deformation as well as the stress relaxation response of these cells were evaluated. Actin filaments were influenced by latrunculin A (LatA) and jasplakinolide (Jas). LatA disrupted actin filaments by sequestering actin monomers thus reducing the pool of polymerisable actin. In contrast, Jas was used to increase actin nucleation and polymerization and consequently reduced actin depolymerization [40–42]. To interfere with cytoskeletal microtubules, cells were treated with nocodazole (Noc) to destabilize microtubules, which consequently promotes their depolymerization. To achieve the contrary effect, paclitaxel (Tax) was used to stabilize microtubules [43]. Within this approach, the contributions of actin filaments and microtubules to the overall cell mechanics were evaluated in a decoupled manner for small and large strains. In contrast to previous work, we were able to separate the contributions of deformation and relaxation to the mechanical properties of cells for actin and microtubule networks for two orders of magnitude of drug dose concentrations. Here, we single out distinctive contributions for cell mechanical changes of the cytoskeleton.

2. Materials and methods

2.1. Cell culture and drug treatment

The MCF-7 cell line was bought from ATCC (ATCC, HTB-22) and were cultured with Mimimal Essential Medium Eagles with L-Glutamine and Earles salt (Biochrom, FG 0325). The cell culture medium was supplemented with 100 mg ml^{-1} Sodium Pyruvate (Sigma-Aldrich, P 5280), 10 μg ml^{-1} Bovine Insuline (Sigma-Aldrich, I6634), 5 ml of Non-essential amino acids (Biochrom, K 0293), 50 ml Fetal Bovine serum (Biochrom, S 0615), and 1 unit of Penincillin/Streptomycin (Biochrom, A 2212).

LatA (Sigma-Aldrich, L5163), Noc (Sigma-Aldrich, M1404) and Tax (T7402) were obtained from Sigma. Jas (Calbiochem, 420107) was bought from Calbiochem. All drugs were dissolved in 1 ml of dimethyl sulfoxide and 100 μg of the dissolved drug was further dissolve in 5 ml of culture medium. From this, the necessary volume was added to the cells while adherent to obtain the needed concentrations. Cells were incubated with Tax for 18, 10 h for Noc, and 6 h for Jas. LatA, was added to the cells in suspension 2 min before they were measured, thus the cells were measured in a LatA containing medium.

2.2. Automated microfluidic OS

The setup is as described in [39] with minor changes such as the microfluidic and stretching processes being computer controlled. A prototype version was provided by RS Zelltechnik GmbH. The mechanical properties of cells were determined by introducing the cells into the automated microfluidic OS where they are serially trapped and stretched. The cell radius along the laser axis is determined while the cell is trapped for a second at

100 mW. The cell is then stretched at 750 or 1200 mW. During the stretch, images are taken at 30 frames per second. The cells are allowed to relax for 2 s after stress cessation. The time-dependent, relative deformation is defined as $[r_t/r_1 - 1]$, where r_t is the cell's diameter at time t and r_t is the cell's diameter when the cell was trapped. Furthermore, the relative relaxation was defined as $[r_t - r_3]/[r_1 - r_3]$, where r_3 is the cell diameter at end of stretch, $t = 3$ s, and r_t is the cell diameter at time t while relaxing, $t > 3$ s. About 1000 cells were measured for each measurement. The relative deformation of the cells in the large strain regime is underestimated because at very large cell deformations ($\geqslant$20%) the edge detection algorithm was unable to capture the cells' edges accurately due to changes in the contrast.

2.3. The effect of cell size on cell deformation

The deformation of cells within the automated microfluidic OS depends sensitively on the ratio of the radius of the laser beam at the centre of the trap and the cell radius [23]. Recent works have shown that cell deformation increases with increasing cell radius [44], while others showed that cell deformation decreased with increasing cell radius [45]. This contradiction shows the difficulty in normalizing data from the stretcher analytically. To avoid this problem in this work, cells of the same radii were compared (see figures S2a, S2b and S3a, available online at stacks.iop.org/NJP/19/093003/mmedia). However, a maximum change of about ± 1 μm was observed in the averaged cell radius for a couple of measurements (see figure S3b). Considering the calculations in [44] and [45], an increase in cell radius of about ± 1 μm would lead to a relative increase in strain of about 5% compared to normal sized cells. That is, if a cell deforms by 0.07%, an increase in its size by 1 μm would lead to a deformation of 0.0735%. This cell size effect is within our error estimation and is therefore not the cause of the changes in deformation observed in this work. It is however noteworthy that the deformation of cells in the automated microfluidic OS is not largely determined by cell radius as pointed out in [45] because their simulations assumed a homogenous optical property of the cells. A plot of the cell radius against the relative deformation does not show any particular trend (see figure S4). This suggests that there are other factors such as cellular heterogeneity, nuclei size and the stage of the cells in the cell cycle influencing cellular deformation.

2.4. Confocal laser scanning microscopy

A mixture (500 μl) containing 250 μl of Nanofectin (GE Life Sciences, Q051-005) and 250 μl GFP E-MAP tubulin and Lifeact mcherry DNA was added drop-wise to the culture medium in a flask containing MCF7 cells. The cells were culture for 24 h after which the cells were washed with PBS, trypsinized, centrifuged and resuspended. The drugs were added at the appropriate times during culture. The cells were allowed to start settling for 20 min. The cells were then observed on the confocal laser scanning microscope while still having a spherical geometry.

2.5. Spinning disc confocal microscopy

Cells were cultured in μ-Plate 96-wells (ibidi, 89626). Cells were rinsed twice with PBS and kept for 30 min in staining solution. Staining solution was made of PBS containing 200 nM Tubulin Tracker™ Green (ThermoFisher, T34075) and 1 μM SiR-DNA (Spirochrome, SC007). Images were taken with inverted Axio Observer.Z1/Yokogawa CSU-X1A 5000 (Carl Zeiss Microscopy GmbH, Jena, Germany), 63x/1.30 Immersion PH3 Objective, lateral resolution of 235 nm and axial resolution of 460 nm for wavelengths of 490 nm. For cell detachment, we added 1:1 Trypsin-EDTA (Sigma, 59417C) and PBS resulting in final concentration of 0.025% Trypsin and 0.01% EDTA.

3. Results

The low strain regime was obtained with a stretch laser power of 750 mW (stress approx. 14 Pa) resulting in a maximum relative deformation below 5% at the end of the stretch (figure 1(a)). Within this regime, a physiological temperature is maintained [46, 47]. For 1200 mW (stress approx. 23 Pa) a high strain regime was achieved with maximum relative deformations beyond 5% (figure 1(d)). The applied stress of the stretch laser was calculated based on ray-optics studies of concentrically placed, spherical shells of different refractive indices as a model of cells with a cortical layer. The calculations are described in detail in Ananthakrishnan *et al* [36] with additional corrections described in Grosser *et al* [48].

Small deformations in the linear regime (up to 5% [49]) are dominated by actin and intermediate filaments [27, 50]. For larger deformations between 5% and 25% strain, nonlinear effects of the actin cytoskeleton can result in nonlinear responses, e.g., strain stiffening [11, 51, 52] and strain softening [53, 54]. The strain response for small laser powers shows a more pronounced viscous response, whereas for high laser powers a more viscoelastic response is distinguishable. However, the initial rapid, irregular deformation, between 1 and 1.5 s, is partially a result of the nuclear thermal instability of the MCF-7 cells [55]. Since we further investigate the

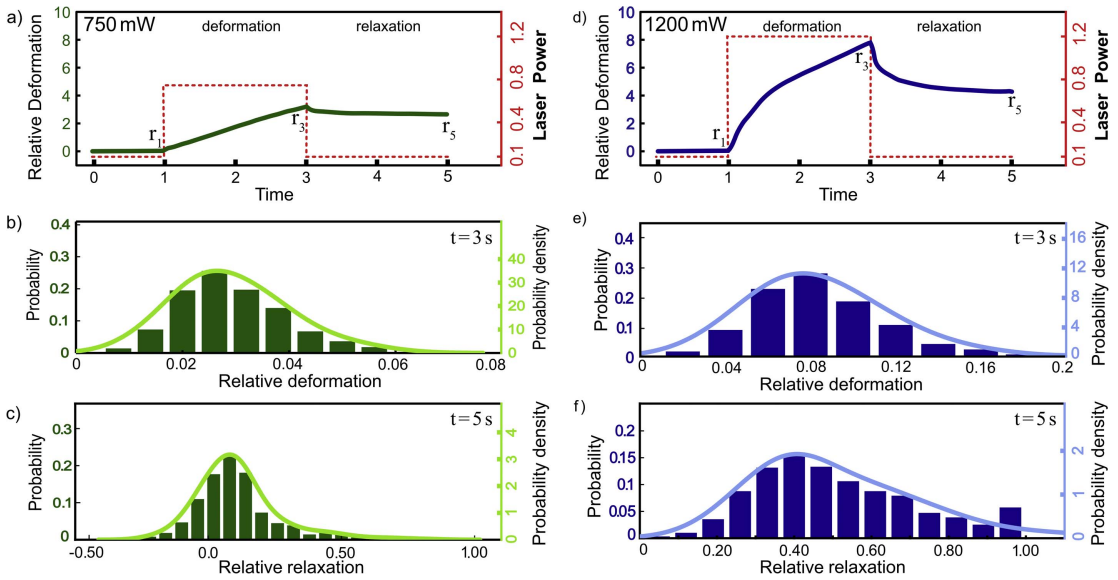

Figure 1. Plots of cells stretched with two different laser powers and the corresponding distributions of the relative deformation and relaxation fitted with the smoothed probability density function. Cells were stretched with a power of 750 mW (a) or 1200 mW (d) for 2 s. The red dashed line indicates the laser power, while the dark green (a) or dark blue (d) is the time-dependent deformation of the cell. (b) Shows the histogram of the relative deformation of cells at small strains and the arising probability density function. The distribution is not completely symmetric, as it would be expected for a normal distribution. (c) The histogram shows the relative relaxation of cells at small strains. The distribution is symmetric as expected for a normal distribution. The minimal optical trapping force (100 mW) of the laser can cause a negative relative relaxation for quasi-viscous mechanical response of cells. Accordingly, for large strains, the histograms of the relative deformation (e) and the relaxation (f) of MCF-7 cells are shown.

cytoskeletal effects of toxins, the induced constant offset in the relative deformation due to nuclear reshaping is not an essential issue in further data analysis.

For small and large strains, we observed asymmetric distributions for the relative deformations at the end of stretch ($t = 3$ s, figures 1(b) and (e)), given as $[r_3/r_1 - 1]$, which broadens for large strains. Furthermore, we define the relative relaxation as a measure of plasticity ($t = 5$ s, figures 1(c) and (f)) as following: $[r_5 - r_3]/[r_1 - r_3]$. The relative relaxation distributions at small strains were symmetric at around $0\% \pm 15\%$ for all measurements (figure 1(c)) but not as broad as the asymmetric relaxation distributions at large strains (figure 1(f)). Since most distributions are asymmetric, the differences in the deformation behaviour of individual cells is not a simple Gaussian function. However, we used a bell curve to calculate the mean and variance of the distributions plotted in the subsequent sections. All comparisons in percentages given in the succeeding sections are done with respect to the relative deformation of untreated cells.

3.1. The impact of actin filaments on cell deformation at small and large strains

At small strains ($\leqslant 5\%$, cells stretched with 750 mW), depolymerization of actin filaments by adding LatA (100 nM) increased the relative deformation of cells up to 75% (figure 2(a)). In contrast to the destabilization, an increased actin nucleation and polymerization due to the addition of Jas resulted in an increase in cell deformation with a maximum increase of about 53% occurring at 200 nM (figure 2(b)).

At large strains ($\geqslant 5\%$, cells stretched with 1.2 W), the disruption of actin filaments led to a maximum increase of 65% in the relative deformation at 1 μM LatA (figure 2(a)), but initiating actin nucleation and polymerization via Jas resulted in no significant change in deformability (figure 2(b)).

3.2. Contribution of actin filaments to cell relaxation

Cell relaxation as considered in this work could also be referred to as the degree of cell plasticity since only a very small percentage of cells relaxed completely in the observation time. Furthermore, at small strains, some cells did not relax while others responded by active elongation. We refer to an active response if the cells expanded after stress release above the maximum deformation during the stretch, i.e. the cells displayed a positive slope in the last second of relaxation resulting in a negative relaxation value. Since these relaxation behaviours cannot be found in an isotropic viscoelastic material, we suspect that this behaviour is caused by active cellular processes such as restructuring of the cytoskeleton [8] and the predominant viscous response in the small strain regime.

The disruption of actin filaments or the enhanced initiation of nucleation and polymerization resulted in the active behaviour of cells at small strains as shown by the negative relaxation values in figures 2(c) and (d). At large strains, this disruption led to a significant decrease in cell relaxation of 32% at 1 μM of LatA (figure 2(c)) implying

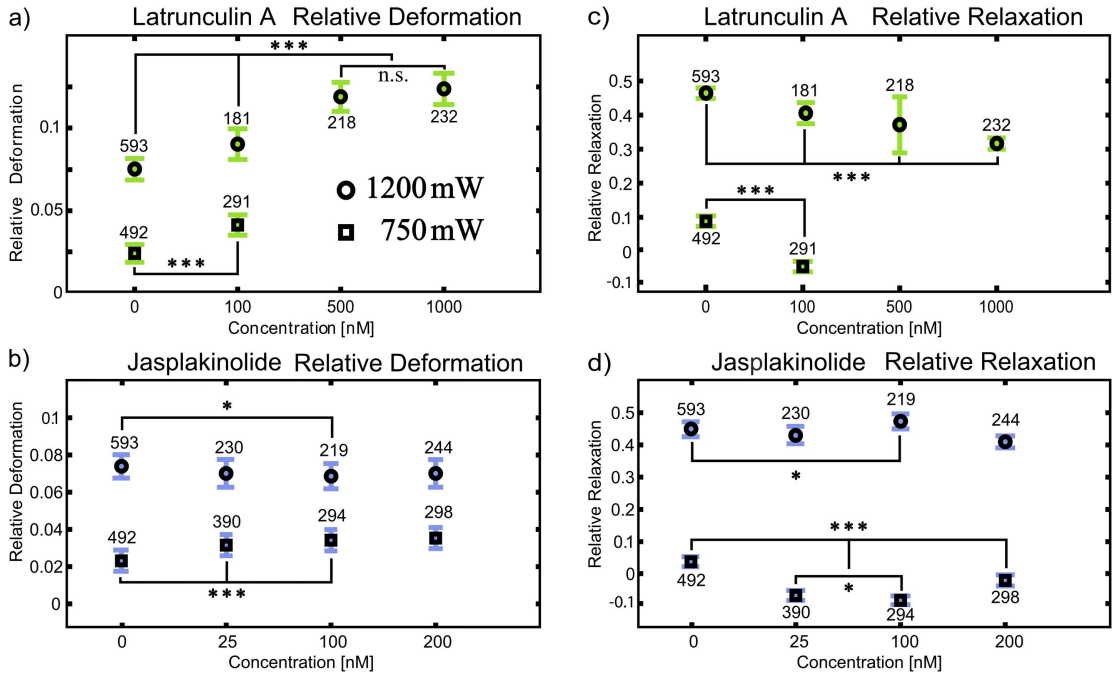

Figure 2. Relative deformation and relaxation of MCF-7 cells treated with latrunculin A and jasplakinolide, respectively. The black circles are the relative deformation at large strains (cells stretched at 1.2 W), while the squares are for the small strains (cells stretched at 750 mW), mean ± (SEM + reproducibility variance). The reproducibility variance was obtained by measuring the cells twice per passage number and for two different passages numbers. The number above each point on the plot is the number of cells from which the mean was obtained. Asterisks indicate the level of significance of the two-sided Kolmogorov–Smirnov test with $p < 0.05$, $p < 0.01$, $p < 0.001$ for one, two and three asterisks, respectively. Branched indicators for significance denote significance between all pairs of included measurements. Sub-branches indicate a lower level of significance between the two samples of the sub-branch. No asterisks denote samples with no significance compared to control measurement. (a) Shown are the relative deformation of LatA treated cells for small (squares) and large (circles) strains. The relative deformation increased significantly with increasing LatA concentration for both small and large strains. An increase from 500 to 1000 nM did not significantly increase the relative deformation. (b) Relative deformations of Jas treated cells for small (squares) and large (circles) strains are displayed. Cell deformation increased substantially with increasing Jas concentration for small strains and concentrations up to 100 nM and showed no significant change at large strains. (c) The relative relaxation, mean ± SEM, of LatA treated cells are illustrated. At small strains (squares), the cells are actively elongating, while at large strains (circles), the cells become significantly more plastic with increasing LatA concentration. (d) The relative relaxation of Jas treated cells revealed that cells actively elongate at small strains (squares) and showed no significant change at large strains (circles).

that the cells became more plastic. In contrast, the enhanced initiation of actin nucleation and polymerization had no significant effect on cell relaxation for all concentrations for measurements at large strains (figure 2(d)).

3.3. The impact of microtubules on cell deformation at small and large strains

As shown in (figure 3(a)) for small strains, disrupting the microtubules by adding Noc (ranging from 1 to 20 μM) had no significant effect on the relative deformation of cells. Stabilizing microtubules using Tax (25 nM to 4 μM) did not affect the relative deformation at small strains either (figure 3(b)).

At large strains, the disruption of microtubules caused by Noc (ranging from 1 to 10 μM) induced no significant change in cell deformation. At 20 μM Noc, however, a significant increase of 20% was observed (figure 3(a)). Stabilization of microtubules via Tax revealed a bipolar effect for measurements at large strains. For low concentrations, cells initially softened, but subsequently the cell populations stiffened for higher Tax concentrations. From 25 to 100 nM, the relative deformation increased by about 32%. The deformation decreased to its original value at 200 nM and remained constant from this concentration to 500 nM. Increasing the concentration from 500 nM to 2 μM Tax resulted in cell stiffening yielding a decrease of about 40% in relative deformation (figure 3(b)).

3.4. Contribution of microtubules to cell relaxation

At small strains, the disruption of microtubules resulted in a significant decrease of 70% in cell relaxation at 20 μM of Noc (figure 3(c)). The stabilization of microtubules in this regime showed no significant effect up to 0.5 μM Tax. However, from 1 μM onwards, cells relaxed actively and expanded after stress release (figure 3(d)). At large strains, microtubule disruption resulted in a decrease in relaxation of about 23% at 20 μM Noc (figure 3(c)) while microtubule stabilization led generally to a decrease in relaxation reaching a maximum of 30% at 50 nM Tax (figure 3(d)).

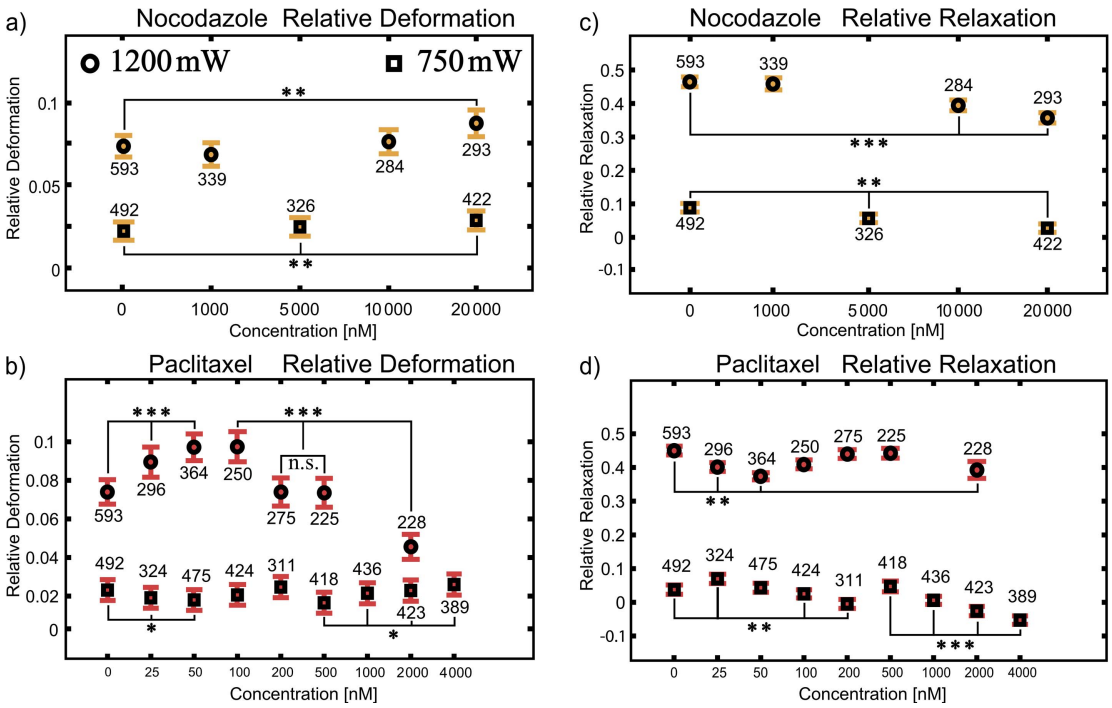

Figure 3. Relative deformation and relaxation of MCF7 cells treated with nocodazole and paclitaxel. The black circles are the relative deformation at large strains (cells stretched at 1.2 W) while the squares are the small strains (cells stretched at 750 mW), mean ± (SEM + reproducibility variance). Asterisks indicate the level of significance of the two-sided Kolmogorov–Smirnov test with $p < 0.05$, $p < 0.01$, $p < 0.001$ for one, two and three asterisks, respectively. Branched indicators for significance denote significance between all pairs of included measurements. Sub-branches indicate a lower level of significance between the two samples of the sub-branch. No asterisks denote measurements with no significance compared to the control measurement. (a) The relative deformation of Noc treated cells is shown. At small strains (squares), Noc was ineffective for all concentrations and displayed only a subtle trend towards higher deformability for increasing concentration. At large strains (circles), a significant increase in cell deformation was only observed at 20 μM Noc. (b) The relative deformation of Tax treated cells revealed no significant overall trend for small strains (squares). For low concentrations, the deformability approaches lower values whereas for higher concentrations, the cells become more deformable again. However, both trends have no considerable impact of cell mechanics. At large strains, the effect of Tax was bipolar and concentration dependent. From 25 to 100 nM Tax, an increase in relative deformation was observed. Above 100 nM, the relative deformation decreased. (c) The relative relaxation of Noc treated MCF7 cells shows that the cells became significantly more plastic at small (squares) and large (circles) strains. (d) The relative relaxation of Tax treated cells is illustrated. At small strains (squares), cellular plasticity increased with increasing concentration and the cells actively elongate from 1 μM Tax and higher concentrations. At large strains (circles), cellular plasticity increased generally but was pronounced at smaller concentration of Tax.

4. Discussion

In suspension, cells develop a well-defined spherical geometry, free of visible stress fibres with the actin cytoskeleton forming an cortex-like structure which spans the entire cell [56]. Moreover, the microtubules network shows a surprising picture by not clearly indicating whether the microtubules emanate from the microtubule-organizing centre (figure 4). The microtubules form a random network at the cells' interior and pronounced bundles at the periphery (figure 4(a)). This aligned peripheral bundling may be due to collective buckling at the cells' boundary. This is in contrast to the radially outward pointing network found in adherent cells. Microtubules have been shown to have a length-dependent persistence length [57] ranging from 5 to 100 μm, which is substantially stiffer than other cytoskeletal filaments. Therefore, the bending of microtubules within cells emphasizes the presence of compressive forces. We would like to note that local bending can be also induced by forces exerted by active molecular motors or passive cross-linking effects [58, 59]. However, these processes cannot sufficiently explain how several microtubules are bent in parallel, which further indicates the presence of compressive forces. Nevertheless, it remains unclear whether the plasma membrane or the actin cortex can generate such counteracting forces, but previous studies suggested the latter case [60, 61].

The used high concentrations of toxins refer to clinical relevant dosages; whereas a saturated cytotoxicity is strongly preferred, see figure 5. Many toxins, e.g. Tax, show less pronounced toxicity for lower concentrations (figure 5 below 25 nM). Nonetheless, this regime is of interest for fundamental research to investigate functional details of cellular or cytoskeletal structures, respectively [62]. Studying the accumulation dynamics of Tax, for instance, can reveal new insights for cancer diagnostics since it has a high binding affinity to microtubules and accumulates differently in different cell types, pronounced in malignant cells [62–65].

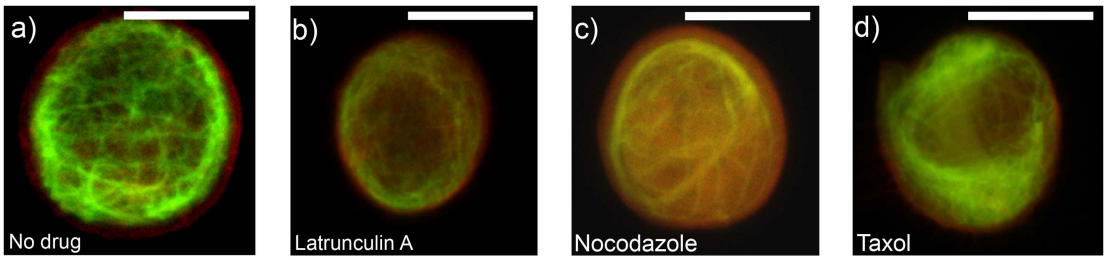

Figure 4. Confocal laser scanning images of MCF-7 cells in suspension showing GFP stained microtubules and RFP stained actin filaments (scale bars 5 μm). The green filaments are the microtubules while the red represents the actin meshwork. (a) In an untreated cell microtubules are highly bend and concentrated at the cell's periphery but form a random network at the cell's interior. Actin is spread throughout the cell. Both microtubules and actin form a cortex at the periphery. (b) A cell was treated with 500 nM LatA to disrupt actin filaments. The microtubule network is maintained as in the non-treated cell with less pronounced actin filaments spread across the entire cell. (c) A cell was treated with 20 μM Noc to disturb microtubules. Actin filaments are spread across the cell and the microtubules network is reduced. Nevertheless, a concentrated region at the cell's periphery is sustained. (d) A cell treated with 2 μM Tax displays a dense network of aligned microtubules along the cell periphery and actin filaments spread throughout the entire cell.

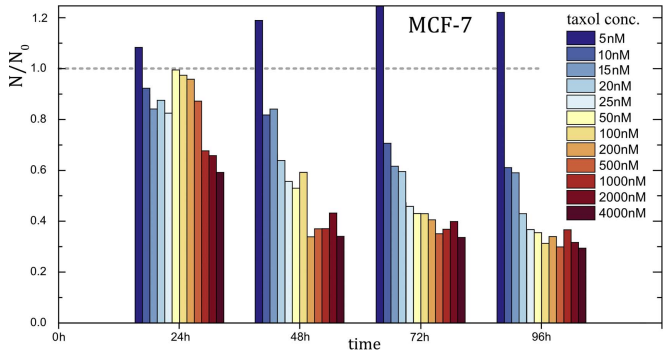

Figure 5. Cytotoxicity Assay for different Tax concentrations for an exposure time of 4 d. Paclitaxel stabilizes microtubules and hinders cell division. For concentrations beyond 25 nM and exposure times of 3 d and more, the toxicity is not majorly increased and nearly independent of the concentration. Below 500 nM, paclitaxel shows a pronounced lag time in its toxicity for the first 24 h. Comparable low concentrations of 5 nM lead to strongly decreased proliferation rates. The doubling time of MCF-7 with no Tax was determined to (38.8 ± 4.2) h. Since the cytotoxicity mainly arises from disrupted cell division and arresting cells in M-phase, only a fraction of cells, which have entered mitosis, are strongly affected by Tax.

In the low concentration regime, a lag time in the cytotoxic effect can be observed. The doubling time, and therefore cell cycle time, is approx. 39 h. Only fractions of cells have entered mitosis and are subject to a major cytotoxic effect of Tax. However, Tax is also toxic in the interphase [66, 67] and solely the mitotic index is not sufficient to explain the efficacy [64]. For concentrations ranging from 80 to 280 nM, Tax is reported to kill tumour cells by inducing multipolar divisions [68] (see supplementary figure S5). Subsequently, the aneuploidy daughter cells will eventually die due to cytokinesis failure and chromosome missegregation [64, 68].

Higher concentrations of Tax (200 nM and above) results in higher fractions of cells forced into mitotic arrest instead of dividing multipolar. In accordance with previous research [63, 64, 66–68], the induced mitotic arrest explains the observed rapidly saturated cytotoxicity for long exposure times. The cytotoxicity is also independent of the concentration if mitotic arrest is induced in cells (200 nM and above, figures 5 and 6).

4.1. Actin filaments dominate cell response at small strains

At small strains, the disruption of actin filaments led to a significant increase in cell deformation (figure 2(a)). Moreover, initiating enhanced actin nucleation and aggregation [69] resulted in an increase in cell deformation (figure 2(b)). This increase in deformation is most likely caused by a reduction of cross-linked actin filaments (figure 4(b)) since he storage modulus strongly dependents on crosslinking density [70, 71]. While actin has a major influence in this deformation regime, destabilization of microtubules had no significant effect on the overall cell deformation (figure 3(a)). At a first glance, these findings do not agree with previous studies reporting that microtubule destabilization initiated acto-myosin contractions in cultured cells [72] while the stabilization of microtubules inhibited acto-myosin contractions [73]. Additionally, acto-myosin contractions have been shown to induce cortical flows that are capable of generating inward forces leading to cytokinesis [74]. A combination of these findings may explain the ineffectiveness of Noc at small strains (figure 3(a)). The reduction

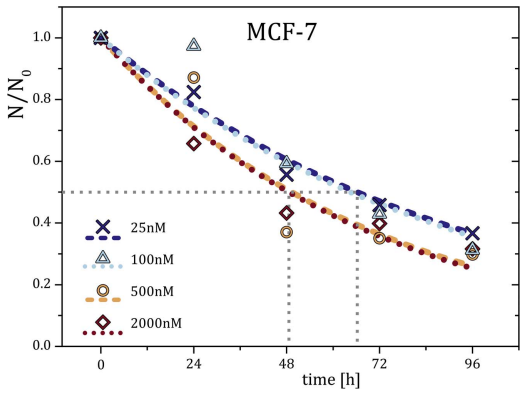

Figure 6. Comparison of time-dependent cytotoxicity of paclitaxel for two orders of magnitude. The dashed and dotted lines are exponential decay fits with toxicological half times (grey dashed lines) in the range of approximately 49–67 h with an SEM of 12 h. For concentrations above 200 nM, the exponential fits show strong deviations for exposure times of 48 h and longer, presumably due to saturation effects and cytotoxic lag times.

in cortical microtubule bundles may be counteracted by strain-hardening effects of the actin filaments caused by increased acto-myosin contractions [75] initiated by microtubule depolymerization. Stabilizing microtubules had no effect on cell deformation at small strains (figure 3(b)) since the imposed stress is not large enough to deform the microtubules within the cytoskeleton. Thus, only the actin cortex is effectively probed. The effect of the stabilized microtubules, however, is indirectly evident as the strengthened microtubules (figure 4(d)) slightly push the actin cortex slightly outwards. The increase in cellular deformation resulting from actin perturbation and the ineffectiveness of microtubule stabilization or disruption suggest that actin filaments alone determine cell mechanics at small strains.

4.2. Microtubules determine cell relaxation at small strains

Cell relaxation at small strains appeared active upon initiating enhanced actin nucleation and surprisingly upon destabilization of actin filaments, which is illustrated by the drop of the relative relaxation below zero for treated cells (figures 2(a) and (b)). In contrast, control cells without drug-induced cytoskeletal perturbations remained inactive displaying a positive value for the relative relaxation (figures 2(a) and (b)). The mechanical properties of actin structures have been shown to dependent on the cross-linker dynamics [70, 76–78], which highlights that stretching cells breaks cross-linkers such as filamin and α-actinin [24]. The weakening of physical inter-filament coupling increases the contribution of viscous deformations and consequently a decrease of elastic contributions since the percolation of the cross-linked network is decreased [70, 79]. Thus, contractile restoring forces are less effectively transmitted through the structure resulting in an increase in cell plasticity. Moreover, microtubules have been shown to buckle upon the active, highly contracting actin cortex during their polymerization [60, 61] (see figure 4). Stress-induced weakening of the actin cytoskeleton by cross-linker breakage suggests that the active behaviour of the entire cell may result from the slow unbuckling of microtubules. In turn, this suggests an entropic origin of the effect, which has been previously reported for both actin and microtubules [58, 78, 80–84]. Destabilizing microtubules resulted in a lack of relaxation, i.e. an increase in plasticity, especially at very high concentrations of Noc. As shown in figure 4(c), Noc treatment resulted in a reduced but aligned network of microtubules within the cells. This emphasizes that the actin cortex does not only cover the restoring force at small strains. The pressure of buckled microtubules also acts as a restoring force to a spherical shape, which is reduced if Noc is added. In contrast, stabilizing microtubules with a concentration of up to 0.5 μM Tax resulted in no significant change in relaxation (figure 3(d)). Beyond 0.5 μM, the cells became more plastic. This increase in plasticity could also result from the unbuckling of microtubules induced by the applied stress in conjunction with microtubule stiffening by Tax treatment. Furthermore, microtubule networks have been shown to release stress over very long times [85], which might explain the general increase in cell plasticity after the stretch.

4.3. Actin filaments and microtubules equally contribute to cell mechanics at large strains

At large strains, disrupting the actin filaments resulted in a significant increase in cell deformation. This increase stems from the loss of mechanical integrity of the actin cytoskeleton and agrees with many reports in literature [7, 24, 25].

The role of the microtubules to cell mechanics has previously often been ignored or underestimated. While the actin cortex is a major contributor to cellular mechanics and stiffness [56], we want to point out that also the microtubule network forms a cortex in suspended state of cells (see figure 7).

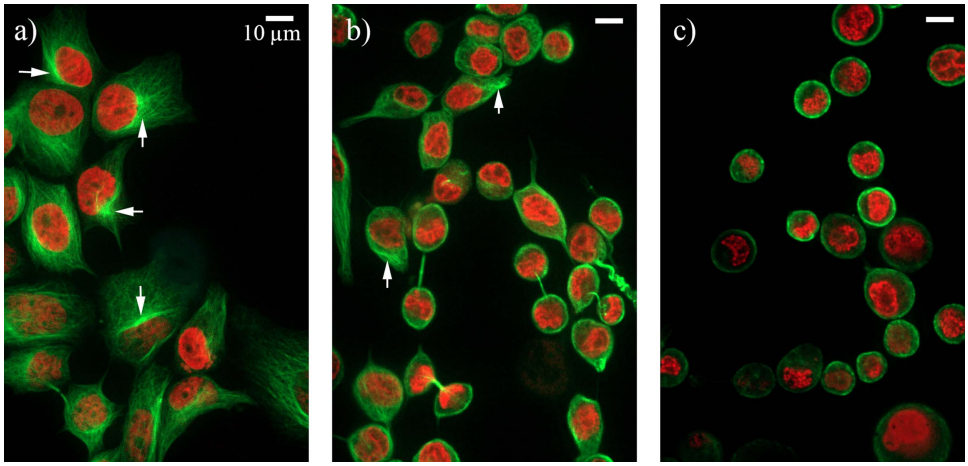

Figure 7. Time series of spinning disc microscope images of cells under influence of low concentration of trypsin-EDTA (0.025%). Microtubules stained in green (Tubulin Tracker Green) and nucleus stained in red (SiR-DNA). (a) Before adding trypsin, cells have well-structured microtubule networks with a microtubule organizing centre (MTOC, white arrows). Microtubule density decreases towards the cell membrane. (b) After 10 min of trypsination, the MTOC is barely recognizable and microtubules start to form a cortex-like structure [56]. (c) After complete detachment from the substrate, the MTOC has dissolved and major parts of the microtubules have formed a microtubule cortex.

Microtubule destabilization increased the overall cell compliance, which is only significant at very high Noc concentrations (figure 3(a)). Noc reduces the microtubule concentration and consequently weakens the observed microtubule network structure (see figure 4(c)) leading to a reduced cell stiffness [85]. These increments in deformation upon destabilizing of both actin filaments and microtubule point towards a cooperative working principle to regulate cellular mechanics at large strains. The initiation of enhanced actin nucleation did not affect the cell deformation. *In vitro* studies showed that actin networks rupture at relatively low strains at constant stress [85]. Therefore, the role of the actin filaments at large strains is negligible while the contributions of other filaments such as the intermediate filaments or microtubules become dominant.

4.4. Stabilizing microtubules has a bipolar effect on cell mechanics at large strains

Stabilizing microtubules by Tax treatment has a concentration-dependent bipolar effect with an increase in deformation at small concentrations of Tax and a decrease at larger concentrations of Tax (figure 3(b)). Microtubule polymerization imposes an outward force on the cell by forming a scaffold, which impedes dynamic instabilities. Thus, their stabilization maintains this imposed force and consequently make cells more compliant. Furthermore, stabilizing microtubules inhibits acto-myosin contractions [73], which oppose cell deformation. From 200 nM onwards, however, cells are stiffened with an effectiveness peaks at 2 µM. This stiffening could be initiated by stabilized microtubules pushing the actin cortex outward to a point where it strain-hardens. Since 200 nM of Tax is approximately the threshold concentration for mitotic arrest, we cannot exclude that cell cycle dependent effects may also play a role. Beyond 2 µM, cells literally explode when higher forces are applied on them (see supplemented video).

4.5. Actin filaments and microtubules both regulate cell relaxation at large strains

Destabilizing actin filaments decreased the cellular relaxation while initiating enhanced actin nucleation had no significant effect (figures 2(c) and (d)). This decline in relaxation originates from a reduction in the elastic strength of the actin cytoskeleton leading to an increased viscous response. Moreover, stabilizing and destabilizing microtubules led to an increased in plasticity (figures 3(c) and (d)). This could result from the disruption of the force balance between the actin cortex and outward pushing buckled microtubule. These large deformations resulting from the high optical forces could also decouple the microtubules from the actin cortex by breaking actin-microtubule crosslinker or actin filaments in general. On the other hand, at large strains, microtubules may no longer be bent and thereby losing their original structural role due to an outstretched configuration, which could lead to an increase in plasticity.

4.6. Different onset of affine and non-affine deformations

To understand the varying effects of the two networks under different strains, we like to emphasize that actin filaments and microtubules are inherently structurally and mechanically different, which is especially reflected in their different persistence lengths [8]. In a more generalized frame, cross-linked networks behave differently than purely entangled networks and cross-linker as well as filament concentrations and length scale distribution

have a rather large impact on the overall network stiffness [71, 86–89]. These concentrations as well as the stiffness of a network's components and their arrangements determine the onset of affine or non-affine deformations, which is consequentially different for actin and microtubule networks. Resulting entropic and enthalpic contributions to mechanical properties can substantially vary for these different networks. It has been stated previously that these differences allow cells to regulate their mechanical responses only by small alterations of cross-linker or filament concentrations to precisely alter the mechanical properties of the cytoskeleton [71]. Gardel *et al* even hypothesized that cell mechanics may vary as a function of external prestress and small variation in force can yield different mechanical responses [71]. Since cellular networks of actin filaments and microtubules substantially vary in all different parameters, their transition from affine to non-affine deformations will be different. While affine deformations of the actin cytoskeleton may govern cell responses in the low strain regime, its dominance is decreased for large strains due to the transition to non-affine deformations resulting in a reduced elastic modulus [90]. Within the range of the used large strains, the microtubule meshwork may still be probed in the affine regime and their mechanical response increases with larger deformations dominating the response of the entire system. Consequently, the ratio of contributions from actin networks and microtubule structures are shifted when probing cells with increasing strains yielding cooperativity effects for the arising mechanical properties.

5. Conclusion

Cells were measured in the suspended state and displayed different morphologies than in the adhered case. Microtubules were shown to form apparent random networks instead of pointing outwards radially from the microtubule organizing centre and actin stress fibres were completely absent. In the suspended state, the microtubule network forms a cortex-like shell in analogy to actin networks of suspended cells. Thus, the mechanical fingerprints of suspended cells have to be clearly distinguished from adhered cells.

By employing cytoskeletal drugs, we have been able to identify the distinct roles of actin filaments and microtubules during deformation of suspended cells. In the case of small strains ($\leqslant 5\%$), the cell deformation is mainly dominated by actin structures and the subsequent relaxation is mainly governed by microtubules due to the initiation of an active cell behaviour. In contrast, at large strains ($>5\%$), we found that actin filaments and microtubules cooperated in maintaining cellular integrity. While the influence of actin filaments appeared minor, microtubules became increasingly dominant upon Tax stabilization. This stabilization yielded concentration dependent, bipolar effects on cell deformation. Here, high Tax concentrations refer to clinical relevant dosage where cytotoxic effects dramatically change a cell's structure and mechanics. A lower dose is especially suitable to study and understand the specific roles of the cytoskeletal components.

In the final case, both actin and microtubules were shown to be responsible for cellular relaxation at large strains. With the implication of microtubules facilitating tumour cell attachment during metastasis by use of microtentacles, the bipolar effect of Tax on cell deformation could help explain the increase in circulating tumour cells in blood when taxane treatment was applied before surgery [91]. To further elucidate the role of these cytoskeletal components, including that of intermediate filaments on cell mechanics, the dynamic change in these filaments during stretching has to be accounted for.

Acknowledgments

We like to thank Tobias R Kießling for fruitful discussions and solving programming problems. We acknowledge funding from the European Commission H2020-PHC-2015-two-stage in the frame of the 'FORCE' project. This work has been supported through the Fraunhofer Attract project 601 683. We acknowledge support from the German Research Foundation (DFG) and University of Leipzig within the program of Open Access Publishing.

Author contributions

DKN, HK, JS, RS, and JAK designed research; DKN, HK and EW performed experiments; DKN, HK and JS analysed data; RS provided analytic tools; DKN, HK, JS and JAK wrote the article.

References

[1] Guck J *et al* 2005 Optical deformability as an inherent cell marker for testing malignant transformation and metastatic competence *Biophys. J.* **88** 3689–98

[2] Suresh S, Spatz J, Mills J P, Micoulet A, Dao M, Lim C T, Beil M and Seufferlein T 2005 Connections between single-cell biomechanics and human disease states: gastrointestinal cancer and malaria *Acta Biomaterialia* **1** 15–30

[3] Ingber D E 1990 Fibronectin controls capillary endothelial cell growth by modulating cell shape *Proc. Natl Acad. Sci. USA* **87** 3579–83
[4] Nnetu K D, Knorr M, Käs J and Zink M 2012 The impact of jamming on boundaries of collectively moving weak-interacting cells *New J. Phys.* **14** 115012
[5] Nnetu K D, Knorr M, Strehle D, Zink M and Käs J A 2012 Directed persistent motion maintains sheet integrity during multi-cellular spreading and migration *Soft Matter* **8** 6913
[6] Nnetu K D, Knorr M, Pawlizak S, Fuhs T and Käs J A 2013 Slow and anomalous dynamics of an MCF-10A epithelial cell monolayer *Soft Matter* **9** 9335
[7] Lautenschläger F, Paschke S, Schinkinger S, Bruel A, Beil M and Guck J 2009 The regulatory role of cell mechanics for migration of differentiating myeloid cells *Proc. Natl Acad. Sci.* **106** 15696–701
[8] Huber F, Schnauss J, Rönicke S, Rauch P, Müller K, Fütterer C and Käs J 2013 Emergent complexity of the cytoskeleton: from single filaments to tissue *Adv. Phys.* **62** 1–112
[9] Gupta G P and Massague J 2006 Cancer metastasis: building a framework *Cell* **127** 679–95
[10] Stamenovic D, Mijailovich S M, Tolic-Norrelykke I M, Chen J and Wang N 2002 Cell prestress: II. Contribution of microtubules *Am. J. Physiol. Cell Physiol.* **282** C617–24
[11] Wang N, Tolic-Norrelykke I M, Chen J, Mijailovich S M, Butler J P, Fredberg J J and Stamenovic D 2002 Cell prestress: I. Stiffness and prestress are closely associated in adherent contractile cells *Am. J. Physiol. Cell Physiol.* **282** C606–16
[12] Wang N 1998 Mechanical interactions among cytoskeletal filaments *Hypertension* **32** 162–5
[13] Hoffman B D, Massiera G, van Citters K M and Crocker J C 2006 The consensus mechanics of cultured mammalian cells *Proc. Natl Acad. Sci. USA* **103** 10259–64
[14] Rotsch C and Radmacher M 2000 Drug-induced changes of cytoskeletal structure and mechanics in fibroblasts: an atomic force microscopy study *Biophys. J.* **78** 520–35
[15] Lam W A, Rosenbluth M J and Fletcher D A 2007 Chemotherapy exposure increases leukemia cell stiffness *Blood* **109** 3505–8
[16] Dudani J S, Gossett D R, Tse H T K and Di Carlo D 2013 Pinched-flow hydrodynamic stretching of single-cells *Lab Chip* **13** 3728–34
[17] Gossett D R, Tse H T, Lee S A, Ying Y, Lindgren A G, Yang O O, Rao J, Clark A T and Di Carlo D 2012 Hydrodynamic stretching of single cells for large population mechanical phenotyping *Proc. Natl Acad. Sci. USA* **109** 7630–5
[18] Mietke A, Otto O, Girardo S, Rosendahl P, Taubenberger A, Golfier S, Ulbricht E, Aland S, Guck J and Fischer-Friedrich E 2015 Extracting cell stiffness from real-time deformability cytometry: theory and experiment *Biophys. J.* **109** 2023–36
[19] Otto O *et al* 2015 Real-time deformability cytometry: on-the-fly cell mechanical phenotyping *Nat. Methods* **12** 199–202
[20] Lange J R, Steinwachs J, Kolb T, Lautscham L A, Harder I, Whyte G and Fabry B 2015 Microconstriction arrays for high-throughput quantitative measurements of cell mechanical properties *Biophys. J.* **109** 26–34
[21] Roth K B, Neeves K B, Squier J and Marr D W M 2016 High-throughput linear optical stretcher for mechanical characterization of blood cells *Cytometry* A **89** 391–7
[22] Guck J, Ananthakrishnan R, Mahmood H, Moon T J, Cunningham C C and Käs J A 2001 The optical stretcher: a novel laser tool to micromanipulate cells *Biophys. J.* **81** 767–84
[23] Guck J, Ananthakrishnan R, Moon T J, Cunningham C C and Käs J A 2000 Optical deformability of soft biological dielectrics *Phys. Rev. Lett.* **84** 5451–4
[24] Wottawah F, Schinkinger S, Lincoln B, Ananthakrishnan R, Romeyke M, Guck J and Käs J A 2005 Optical rheology of biological cells *Phys. Rev. Lett.* **94** 98103
[25] Collinsworth A M, Zhang S, Kraus W E and Truskey G A 2002 Apparent elastic modulus and hysteresis of skeletal muscle cells throughout differentiation *Am. J. Physiol. Cell Physiol.* **283** C1219–27
[26] Heidemann S R and Wirtz D 2004 Towards a regional approach to cell mechanics *Trends Cell Biol.* **14** 160–6
[27] Seltmann K, Fritsch A W, Käs J A and Magin T M 2013 Keratins significantly contribute to cell stiffness and impact invasive behavior *Proc. Natl Acad. Sci. USA* **110** 18507–12
[28] Thoumine O and Ott A 1997 Time scale dependent viscoelastic and contractile regimes in fibroblasts probed by microplate manipulation *J. Cell Sci.* **110** 2109–16
[29] Desprat N, Richert A, Simeon J and Asnacios A 2005 Creep function of a single living cell *Biophys. J.* **88** 2224–33
[30] Trickey W R, Lee G M and Guilak F 2000 Viscoelastic properties of chondrocytes from normal and osteoarthritic human cartilage *J. Orthopaedic Res.* **18** 891–8
[31] Ofek G, Wiltz D C and Athanasiou K A 2009 Contribution of the cytoskeleton to the compressive properties and recovery behavior of single cells *Biophys. J.* **97** 1873–82
[32] Gyger M, Stange R, Kiessling T R, Fritsch A, Kostelnik K B, Beck-Sickinger A G, Zink M and Käs J A 2014 Active contractions in single suspended epithelial cells *Eur. Biophys. J.* **43** 11–23
[33] Nawaz S, Sanchez P, Bodensiek K, Li S, Simons M and Schaap I A T 2012 Cell visco-elasticity measured with AFM and optical trapping at sub-micrometer deformations *PLoS One* **7** e45297
[34] Schlosser F, Rehfeldt F and Schmidt C F 2015 Force fluctuations in three-dimensional suspended fibroblasts *Phil. Trans. R. Soc.* B **370** 20140028
[35] Janmey P A, Euteneuer U, Traub P and Schliwa M 1991 Viscoelastic properties of vimentin compared with other filamentous biopolymer networks *J. Cell Biol.* **113** 155–60
[36] Ananthakrishnan R, Guck J, Wottawah F, Schinkinger S, Lincoln B, Romeyke M, Moon T and Käs J A 2006 Quantifying the contribution of actin networks to the elastic strength of fibroblasts *J. Theor. Biol.* **242** 502–16
[37] Nagayama K and Matsumoto T 2008 Contribution of actin filaments and microtubules to quasi-*in situ* tensile properties and internal force balance of cultured smooth muscle cells on a substrate *Am. J. Physiol. Cell Physiol.* **295** C1569–78
[38] Bow H, Pivkin I, Diez-Silva M, Goldfless S J, Dao M, Niles J C, Suresh S and Han J 2011 A microfabricated deformability-based flow cytometer with application to malaria *Lab Chip* **11** 1065–73
[39] Lincoln B, Wottawah F, Schinkinger S, Ebert S and Guck J 2007 High-throughput rheological measurements with an optical stretcher *Methods Cell Biol.* **83** 397–423
[40] Bubb M R, Spector I, Beyer B B and Fosen K M 2000 Effects of jasplakinolide on the kinetics of actin polymerization. An explanation for certain *in vivo* observations *J. Biol. Chem.* **275** 5163–70
[41] Bubb M R, Senderowicz A M, Sausville E A, Duncan K L and Korn E D 1994 Jasplakinolide, a cytotoxic natural product, induces actin polymerization and competitively inhibits the binding of phalloidin to F-actin *J. Biol. Chem.* **269** 14869–71
[42] Bubb M R 2000 Effects of jasplakinolide on the kinetics of actin polymerization. An explanation for certain *in vivo* observations *J. Biol. Chem.* **275** 5163–70

[43] Rowinsky E K, Cazenave L A and Donehower R C 1990 Taxol: a novel investigational antimicrotubule agent *J. Natl Cancer Inst.* **82** 1247–59
[44] Ekpenyong A E, Posey C L, Chaput J L, Burkart A K, Marquardt M M, Smith T J and Nichols M G 2009 Determination of cell elasticity through hybrid ray optics and continuum mechanics modeling of cell deformation in the optical stretcher *Appl. Opt.* **48** 6344–54
[45] Teo S-K, Goryachev A B, Parker K H and Chiam K-H 2010 Cellular deformation and intracellular stress propagation during optical stretching *Phys. Rev.* E **81** 51924
[46] Kießling T R, Stange R, Käs J A and Fritsch A W 2013 Thermorheology of living cells—impact of temperature variations on cell mechanics *New J. Phys.* **15** 45026
[47] Schmidt B U S, Kießling T R, Warmt E, Fritsch A W, Stange R and Käs J A 2015 Complex thermorheology of living cells *New J. Phys.* **17** 73010
[48] Grosser S, Fritsch A W, Kiessling T R, Stange R and Käs J A 2015 The lensing effect of trapped particles in a dual-beam optical trap *Opt. Express* **23** 5221–35
[49] Wolff L, Fernandez P and Kroy K 2012 Resolving the stiffening-softening paradox in cell mechanics *PLoS One* **7** e40063
[50] Goldman R D, Khuon S, Chou Y H, Opal P and Steinert P M 1996 The function of intermediate filaments in cell shape and cytoskeletal integrity *J. Cell Biol.* **134** 971–83
[51] Pourati J, Maniotis A, Spiegel D, Schaffer J L, Butler J P, Fredberg J J, Ingber D E, Stamenovic D and Wang N 1998 Is cytoskeletal tension a major determinant of cell deformability in adherent endothelial cells? *Am. J. Physiol.* **274** C1283–9
[52] Fernandez P, Pullarkat P A and Ott A 2006 A master relation defines the nonlinear viscoelasticity of single fibroblasts *Biophys. J.* **90** 3796–805
[53] Trepat X, Deng L, An S S, Navajas D, Tschumperlin D J, Gerthoffer W T, Butler J P and Fredberg J J 2007 Universal physical responses to stretch in the living cell *Nature* **447** 592–5
[54] Krishnan R *et al* 2009 Reinforcement versus fluidization in cytoskeletal mechanoresponsiveness *PLoS One* **4** e5486
[55] Warmt E, Kießling T R, Stange R, Fritsch A W, Zink M and Käs J A 2014 Thermal instability of cell nuclei *New J. Phys.* **16** 73009
[56] Salbreux G, Charras G and Paluch E 2012 Actin cortex mechanics and cellular morphogenesis *Trends Cell Biol.* **22** 536–45
[57] Pampaloni F, Lattanzi G, Jonas A, Surrey T, Frey E and Florin E L 2006 Thermal fluctuations of grafted microtubules provide evidence of a length-dependent persistence length *Proc. Natl Acad. Sci. USA* **103** 10248–53
[58] Lansky Z, Braun M, Ludecke A, Schlierf M, ten Wolde P R, Janson M E and Diez S 2015 Diffusible crosslinkers generate directed forces in microtubule networks *Cell* **160** 1159–68
[59] Kent I A, Rane P S, Dickinson R B, Ladd A J C and Lele T P 2016 Transient pinning and pulling: a mechanism for bending microtubules *PLoS One* **11** e0151322
[60] Brangwynne C P, MacKintosh F C, Kumar S, Geisse N A, Talbot J, Mahadevan L, Parker K K, Ingber D E and Weitz D A 2006 Microtubules can bear enhanced compressive loads in living cells because of lateral reinforcement *J. Cell Biol.* **173** 733–41
[61] Brangwynne C P, MacKintosh F C and Weitz D A 2007 Force fluctuations and polymerization dynamics of intracellular microtubules *Proc. Natl Acad. Sci.* **104** 16128–33
[62] Jordan M A, Toso R J, Thrower D and Wilson L 1993 Mechanism of mitotic block and inhibition of cell proliferation by taxol at low concentrations *Proc. Natl Acad. Sci. USA* **90** 9552–6
[63] Jordan M A, Wendell K, Gardiner S, Derry W B, Copp H and Wilson L 1996 Mitotic block induced in HeLa cells by low concentrations of paclitaxel (Taxol) results in abnormal mitotic exit and apoptotic cell death *Cancer Res.* **56** 816–25
[64] Weaver B A 2014 How Taxol/paclitaxel kills cancer cells *Mol. Biol. Cell* **25** 2677–81
[65] Yvon A M, Wadsworth P and Jordan M A 1999 Taxol suppresses dynamics of individual microtubules in living human tumor cells *Mol. Biol. Cell* **10** 947–59
[66] Komlodi-Pasztor E, Sackett D L, Wilkerson J and Fojo T 2011 Mitosis is not a key target of microtubule agents in patient tumors *Nat. Rev. Clin. Oncol.* **8** 244–50
[67] Komlodi-Pasztor E, Sackett D L and Fojo A T 2012 Inhibitors targeting mitosis: tales of how great drugs against a promising target were brought down by a flawed rationale *Clin. Cancer Res.* **18** 51–63
[68] Zasadil L M, Andersen K A, Yeum D, Rocque G B, Wilke L G, Tevaarwerk A J, Raines R T, Burkard M E and Weaver B A 2014 Cytotoxicity of paclitaxel in breast cancer is due to chromosome missegregation on multipolar spindles *Sci. Trans. Med.* **6** 229ra43
[69] Senderowicz A M *et al* 1995 Jasplakinolide's inhibition of the growth of prostate carcinoma cells *in vitro* with disruption of the actin cytoskeleton *J. Natl Cancer Inst.* **87** 46–51
[70] Lieleg O, Claessens M M A E and Bausch A R 2010 Structure and dynamics of cross-linked actin networks *Soft Matter* **6** 218–25
[71] Gardel M L, Shin J H, MacKintosh F C, Mahadevan L, Matsudaira P and Weitz D A 2004 Elastic behavior of cross-linked and bundled actin networks *Science* **304** 1301–5
[72] Kolodney M S and Elson E L 1995 Contraction due to microtubule disruption is associated with increased phosphorylation of myosin regulatory light chain *Proc. Natl Acad. Sci. USA* **92** 10252–6
[73] Danowski B A 1989 Fibroblast contractility and actin organization are stimulated by microtubule inhibitors *J. Cell Sci.* **93** 255–66
[74] Cao L G and Wang Y L 1990 Mechanism of the formation of contractile ring in dividing cultured animal cells: I. Recruitment of preexisting actin filaments into the cleavage furrow *J. Cell Biol.* **110** 1089–95
[75] Alvarado J, Sheinman M, Sharma A, MacKintosh F C and Koenderink G H 2013 Molecular motors robustly drive active gels to a critically connected state *Nat. Phys.* **9** 591–7
[76] Wachsstock D H, Schwarz W H and Pollard T D 1994 Cross-linker dynamics determine the mechanical properties of actin gels *Biophys. J.* **66** 801–9
[77] Strehle D, Schnauss J, Heussinger C, Alvarado J, Bathe M, Käs J A and Gentry B 2011 Transiently crosslinked F-actin bundles *Eur. Biophys. J.* **40** 93–101
[78] Schnauß J, Händler T and Käs J A 2016 Semiflexible biopolymers in bundled arrangements *Polymers* **8** 274
[79] Chelakkot R and Gruhn T 2012 Length dependence of crosslinker induced network formation of rods: a Monte Carlo study *Soft Matter* **8** 11746
[80] Hilitski F, Ward A R, Cajamarca L, Hagan M F, Grason G M and Dogic Z 2015 Measuring cohesion between macromolecular filaments one pair at a time: depletion-induced microtubule bundling *Phys. Rev. Lett.* **114** 138102
[81] Schnauss J, Golde T, Schuldt C, Schmidt B U S, Glaser M, Strehle D, Handler T, Heussinger C and Kas J A 2016 Transition from a linear to a harmonic potential in collective dynamics of a multifilament actin bundle *Phys. Rev. Lett.* **116** 108102
[82] Huber F, Strehle D, Schnauß J and Käs J A 2015 Formation of regularly spaced networks as a general feature of actin bundle condensation by entropic forces *New J. Phys.* **17** 43029
[83] Ellis R 2001 Macromolecular crowding: obvious but underappreciated *Trends Biochem. Sci.* **26** 597–604

[84] Braun M, Lansky Z, Hilitski F, Dogic Z and Diez S 2016 Entropic forces drive contraction of cytoskeletal networks *BioEssays: News Rev. Mol. Cell. Dev. Biol.* **38** 474–81
[85] Lin Y-C, Koenderink G H, MacKintosh F C and Weitz D A 2007 Viscoelastic properties of microtubule networks *Macromolecules* **40** 7714–20
[86] Storm C, Pastore J J, MacKintosh F C, Lubensky T C and Janmey P A 2005 Nonlinear elasticity in biological gels *Nature* **435** 191–4
[87] Broedersz C P and MacKintosh F C 2014 Modeling semiflexible polymer networks *Rev. Mod. Phys.* **86** 995–1036
[88] Schuldt C, Schnauss J, Händler T, Glaser M, Lorenz J, Golde T, Käs J A and Smith D M 2016 Tuning synthetic semiflexible networks by bending stiffness *Phys. Rev. Lett.* **117** 197801
[89] Xu J, Schwarz W H, Käs J A, Stossel T P, Janmey P A and Pollard T D 1998 Mechanical properties of actin filament networks depend on preparation, polymerization conditions, and storage of actin monomers *Biophys. J.* **74** 2731–40
[90] Wen Q, Basu A, Janmey P A and Yodh A G 2012 Non-affine deformations in polymer hydrogels *Soft Matter* **8** 8039–49
[91] Balzer E M, Whipple R A, Cho E H, Matrone M A and Martin S S 2010 Anti-mitotic chemotherapeutics promote adhesive responses in detached and circulating tumor cells *Breast Cancer Res. Treat.* **121** 65–78